European Journal of Medicinal Chemistry 44 (2009) 3601–3611

Contents lists available at ScienceDirect

European Journal of Medicinal Chemistry

journal homepage: http://www.elsevier.com/locate/ejmech

Original article

Identification of putative steroid-binding sites in human ABCB1 and ABCG2

Sergio Mares-Sámano, Raj Badhan, Jeffrey Penny*

University of Manchester, School of Pharmacy & Pharmaceutical Sciences, Stopford Building, Oxford Road, Manchester M13 9PT, UK

ARTICLE INFO

Article history:
Received 13 June 2008
Received in revised form
17 February 2009
Accepted 26 February 2009
Available online 6 March 2009

Keywords:
ABCB1
ABCG2
Homology model
Steroid
Nucleotide-binding domain

ABSTRACT

Homology modelling was used to generate three-dimensional structures of the nucleotide-binding domains (NBDs) of human ABCB1 and ABCG2. Interactions between a series of steroidal ligands and transporter NBDs were investigated using an in silico docking approach. C-terminal ABCB1 NBD (ABCB1 NBD2) was predicted to bind steroids within a cavity formed partly by the P-Loop, Tyr1044 and Ile1050. The P-Loop within ABCG2 NBD was also predicted to be involved in steroid binding. No overlap between ATP- and RU-486-binding sites was predicted in either NBD, though overlaps between ATP- and steroid-binding sites were predicted in the vicinity of the P-Loop in both nucleotide-binding domains.

1. Introduction

P-glycoprotein (ABCB1) and breast cancer resistance protein (ABCG2) limit intracellular drug accumulation by ATP-dependent extrusion of therapeutic agents out of cells. Both proteins are members of the ABC superfamily of transporters and recognise a broad range of drug substrates, including antivirals, antibiotics, calcium channel blockers, and chemotherapeutic drugs used in the treatment of cancer [1–5].

ABCB1 and ABCG2 are expressed at several sites within the body including intestine, liver, kidney and blood–brain barrier and may influence the pharmacokinetic characteristics of therapeutic agents, potentially impacting on treatment efficacy [6–8]. In addition, over-expression of drug efflux transporters in cancer cells is associated with multidrug resistance, a process by which cancer cells acquire resistance to a broad spectrum of structurally and functionally unrelated drugs which leads to poor treatment outcome. ABCB1 and ABCG2 are particularly important since they actively extrude a significant number of therapeutics currently widely used in cancer chemotherapy, including members of the anthracycline, epipodophyllotoxin, vinca alkaloid and taxane drug categories [9–11]. Due to such broad substrate recognition, inhibition of ABCB1 and ABCG2 may potentially improve the treatment efficacy of a range of disease conditions.

The functional unit of ABCB1 and ABCG2 consists of two transmembrane domains (TMDs) and two nucleotide-binding domains (NBDs) [12]. The NBD is responsible for ATP binding and hydrolysis and ABCB1- and ABCG2-mediated drug extrusion is dependent upon two functionally active NBDs. Nucleotide-binding domains contain a number of conserved regions vital to transporter activity. The Walker-A (P-loop) motif is involved in the formation of hydrogen bonds with the inorganic phosphates of ATP and the Walker-B sequence is postulated to be involved in the coordination of Mg^{2+} and in orchestrating the nucleophilic attack on ATP via a water molecule [13]. The role of the Signature sequence remains unclear but it has been suggested to be critical for ATP hydrolysis as well as communication between NBDs and TMDs and conformational change in protein structure associated with substrate translocation across the membrane [14]. Despite these sequences being highly conserved, areas lacking sequence homology are also present within NBDs. Thus, since ATP binding and hydrolysis within NBDs are crucial for maintaining ABCB1 and ABCG2-mediated drug translocation, disruption of these processes is potentially a powerful means of inhibiting transporter activity.

Steroids have been reported to influence multidrug resistance by inhibiting the cellular extrusion of cancer chemotherapeutics [15–18] and studies have revealed steroids are able to bind to abcb1 in the vicinity of the nucleotide-binding domain [19]. The relationship between ATP- and steroid-binding sites within the NBD

Abbreviations: ABC, ATP-binding cassette; BCRP, breast cancer resistance protein; MDR, multidrug resistance; MANT, 2′(3′)-*N*-methylanthraniloyl; NBD, nucleotide-binding domain; PDB, protein data bank; P-gp, P-glycoprotein; TMD, transmembrane domain.

* Corresponding author. Tel.: +44 1612758344; fax: +44 1612758349.
E-mail address: jeffrey.penny@manchester.ac.uk (J. Penny).

0223-5234/$ – see front matter © 2009 Elsevier Masson SAS. All rights reserved.
doi:10.1016/j.ejmech.2009.02.027

has been investigated in in vitro studies in terms of competition and displacement of ATP from recombinant murine P-glycoprotein NBD1. These studies provide evidence that the steroid-binding region in recombinant murine NBD1 appeared to be distinct from the ATP-binding site, although the steroid-binding region is postulated to be adjacent to the ATP-binding site [19].

In an attempt to better define putative steroid-binding sites and understand the mechanisms of steroid interaction with ABCB1 and ABCG2 transporters, we have generated structurally valid in silico homology models of ABCB1 NBD2 and ABCG2 NBD and analysed predicted ligand–NBD interactions. An understanding of the topology of binding sites within the NBDs and of the mechanisms of ligand binding may lead to development of inhibitor drugs targeted to the nucleotide-binding domains of drug efflux transporters.

2. Results

2.1. Selection of templates

A BLAST search revealed that human ABCB1 NBD2 and human ABCG2 NBD protein sequences showed a high level of homology with the NBD regions of other ABC transporters for which the crystal structures were available. ABCB1 NBD2 showed highest sequence identity (48%) with *Escherichia coli* haemolysin B (PDB accession number 1MT0) [20]. The *Lactococcus lactis* ABC transporter NBD (PDB 1MV5) [21], the *Plasmodium yoelii* MDR Protein 2 (PDB 2GH) [22], the Tap1 ATPase domain (PDB ID 2IXF) [23] and the Tap1 C-Terminal domain (PDB 1JJ7) [24] showed between 45% and 46% amino acid identity with ABCB1 NBD2.

ABCG2 NBD demonstrated the highest degree of identity with the *E. coli* Malk protein (31%) (PDB accession number 1Q1B) [25]. The *P. yoelii* MDR Protein 2 (PDB 2GHI) [22], the *E. coli* haemolysin B transporter (PDB 1MT0) [20], the *Sulfolobus solfataricus* glucose ABC transporter (PDB 1OXX) [26] and the *Thermotoga maritima* ABC amino acid transporter (PDB 1VPL) [27] demonstrated between 27% and 28% identity with ABCG2 NBD.

Template sequence identities higher than 25% are accepted to yield good homology models, therefore the templates were used to generate the three-dimensional structures of human ABCB1 NBD2 and human ABCG2 NBD [28].

2.2. Sequence and secondary structure alignments

Multiple sequence alignments of human ABCB1 NBD2 and ABCG2 NBD with their respective templates demonstrated conservation of the integrity and positioning of key sequences associated with ABC-type transporter proteins.

Alignment of ABCB1 NBD2 with template sequences showed that residues within the Walker-A motif (Gly1075, Lys1076, Ser1077, Thr1078), the Walker-B motif (Asp1200, Ala1202, Thr1203, Leu1206, Asp1207) and the Signature sequence Ser1177, Gly1178, Gly1179 were highly conserved, as were the residues within the H-loop (His1257) and within the Q-Loop and Phe1042, Tyr1044, Gly1070, Gly1092, Gly1098, Gln1118, Gly1173, Gly1249 and Gly1255 (Fig. 1). Furthermore, comparison with the template structures revealed that ABCB1 NBD2 secondary structure was composed of ten β-sheets and ten α-helices, accurately reflecting the secondary structures of the template sequences employed (Fig. 1). Alignment of ABCG2 NBD with template sequences showed that residues within the Walker-A motif (Gly85 and Lys86) and the Walker-B motif (Leu210, Asp211) were highly conserved (Fig. 2). Moreover, secondary structure alignment of ABCG2 NBD with the templates demonstrated that the overall folding pattern of ten β-sheets and ten α-helices to be similar to that observed within the nucleotide-binding domain of *E. coli* Malk (Fig. 2).

2.3. Model building

2.3.1. ABCB1 NBD2 homology model

The secondary and tertiary structures of the ABCB1 NBD2 homology model resembled those of the templates used. ABCB1 NBD2 adopts an L-shaped conformation comprised of a two-domain structure, as reported for the *E. coli* haemolysin B transporter [20]. The first domain or Arm I consists of two α-helices and nine β-sheets (Fig. 3a). The conserved motifs of the P-Loop, Walker-B and H-Loop, the anti-parallel β1, β2 sheets and Tyr1024 are located in Arm I, consistent with the structure of Arm I of the *E. coli* haemolysin B transporter. The Q-Loop connects Arm I and Arm II, the latter containing eight α-helices (α1–α8) and the Signature motif, again consistent with the secondary and tertiary structures of the *E. coli* haemolysin B transporter.

2.3.2. ABCG2 NBD homology model

The homology model of the NBD of ABCG2 consisted of two domains and adopted a fold pattern similar to that of the *E. coli* Malk [25]. Arm I exhibits two α-helices and nine β-sheets, which includes the P-Loop, Walker-B, H-Loop, β1, β2, and Phe53. Arm II displays an all α motif and contains the Signature sequence, again consistent with the structure of the *E. coli* Malk (Fig. 3b).

2.4. Stereochemical validation of models

The stereochemical qualities of the protein models were evaluated by means of Ramachandran Plot analysis. 99.2% of the residues of the ABCB1 NBD2 homology model were stereochemically valid and hence were located within the most favoured regions. 99.6% of the residues were within the allowed regions with Lys1164 being the only outlier amino acid. Analyses of the ABCG2 NBD model revealed 95.6% of the residues were within the most favoured regions with 99.6% of the residues in allowed regions; Ser176 was the only amino acid located in an outlier region.

2.5. Prediction of the interaction of steroids with ABCB1 NBD2 and ABCG2 NBD

2.5.1. Identification of ATP-binding sites

To define the ATP-binding sites within human ABCB1 NBD2 and ABCG2 NBD, ATP was docked into the protein homology models. In ABCB1 NBD2, ATP was located within the cavity formed by Tyr1044, the P-Loop and His1232 (Fig. 4a). The α, β and γ phosphate groups of ATP were located within the P-Loop, forming hydrogen bonds with Gly1073, Cys1074, Gly1075, Ser1077, and Thr1078 (Table 1). The adenine ring was stabilised by hydrophobic interactions with Tyr1044 and Gly1073 (Table 1). The predicted docking orientation of ATP was analysed by superimposing the ABCB1 NBD2 homology model onto the structure of the *L. lactis* ABC transporter NBD (PDB ID 1MV5) co-crystallised with ATP. The superpositioning of the two structures revealed overlapping locations of the ATP-binding pockets and confirmed the predicted docking orientation of ATP coincided with the orientation of ATP within the crystal structure (data not shown).

Docking studies with the ABCG2 NBD homology model revealed that ATP was situated in the cavity formed between Phe52, His243 and the P-Loop (Fig. 4b). The α, β and γ phosphate groups of ATP were situated in the P-Loop, forming hydrogen bonds with Gly83, Gly84, Gly85, Lys86, Ser87 and Ser88 (Table 1). The adenine ring was predicted to undergo hydrophobic interactions with Phe52 and several other residues (Table 1). The predicted docking orientation of ATP was investigated by superimposing the ABCG2 NBD homology model onto the *E. coli* Malk protein co-crystallised with ATP [29]. These studies confirmed the location and orientation of

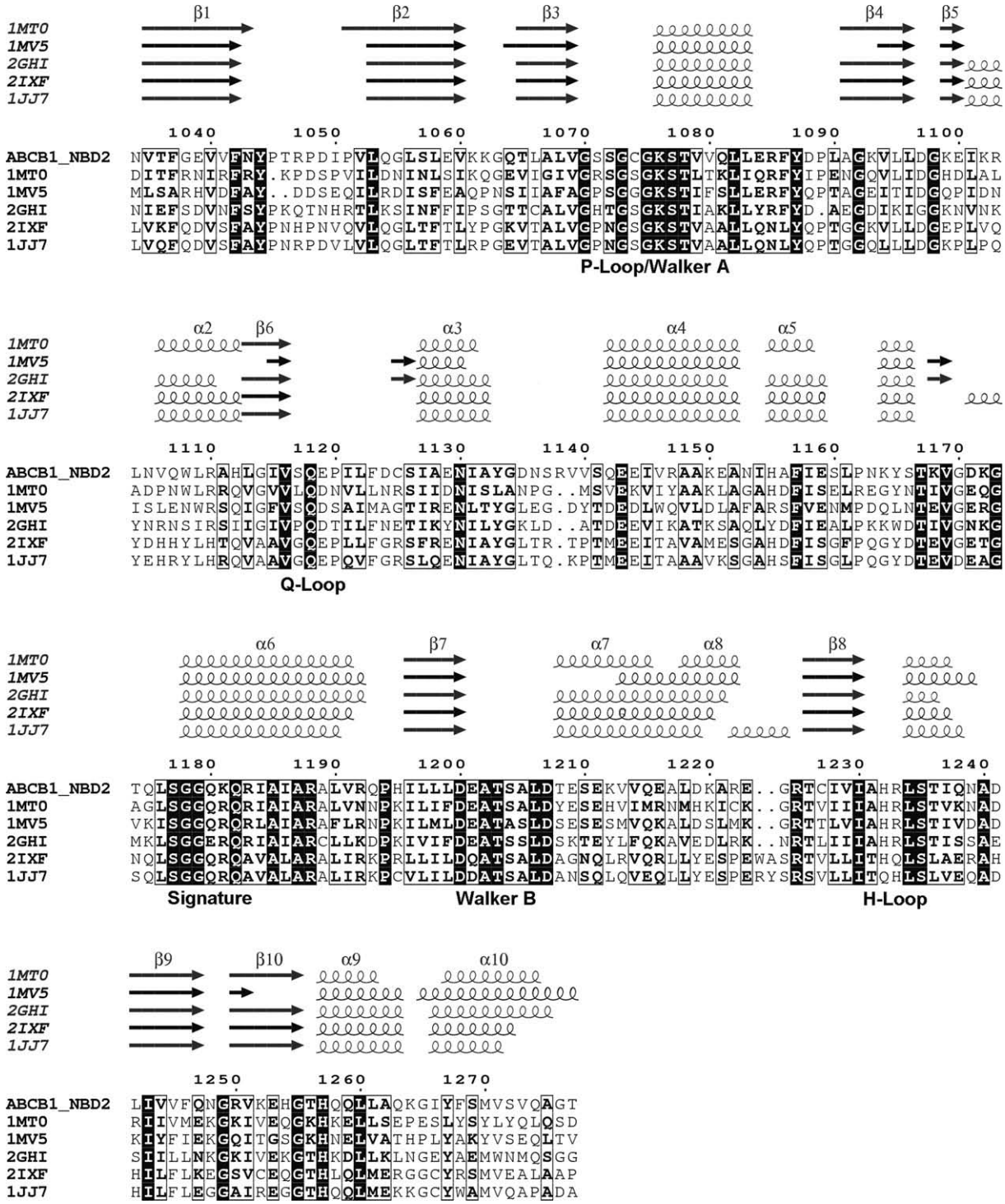

Fig. 1. Multiple sequence alignment of ABCB1 NBD2 and five templates. The nucleotide-binding domains of: *E. coli* haemolysin B (PDB accession number: 1MT0), the *L. lactis* ABC transporter NBD (PDB accession number 1MV5), the *P. yoelii* MDR Protein 2 (PDB accession number: 2GHI), the Tap1 ATPase domain (PDB accession number: 2IXF) and the Tap1 C-Terminal domain (PDB accession number: 1JJ7). Arrows depict β-sheets and helices represent α-helices. Dots represent gaps within the secondary structure prediction. Black shaded blocks represent regions with identical amino acids and grey shaded blocks represent regions with similar amino acids.

ATP docked within ABCG2 NBD coincided with that of ATP within the crystal structure (data not shown).

2.5.2. Identification of putative steroid-binding sites

Previous studies have attempted to characterise the steroid-binding regions of recombinant NBD1, extended-NBD1 and NBD2 of murine abcb1 by analysing tryptophan intrinsic fluorescence in competitive binding assays [19,30,31]. These studies utilised ATP, 2′(3′)-*N*-methylanthraniloyl-ATP (MANT-ATP), the hydrophobic steroid RU-486 and a series of steroids and flavonoids to identify steroid-binding regions within the nucleotide-binding domains. In comparative studies we have employed these agents in in silico docking studies in an attempt to map nucleotide-binding sites and steroid-binding sites within human ABCB1 NBD2 and ABCG2 NBD.

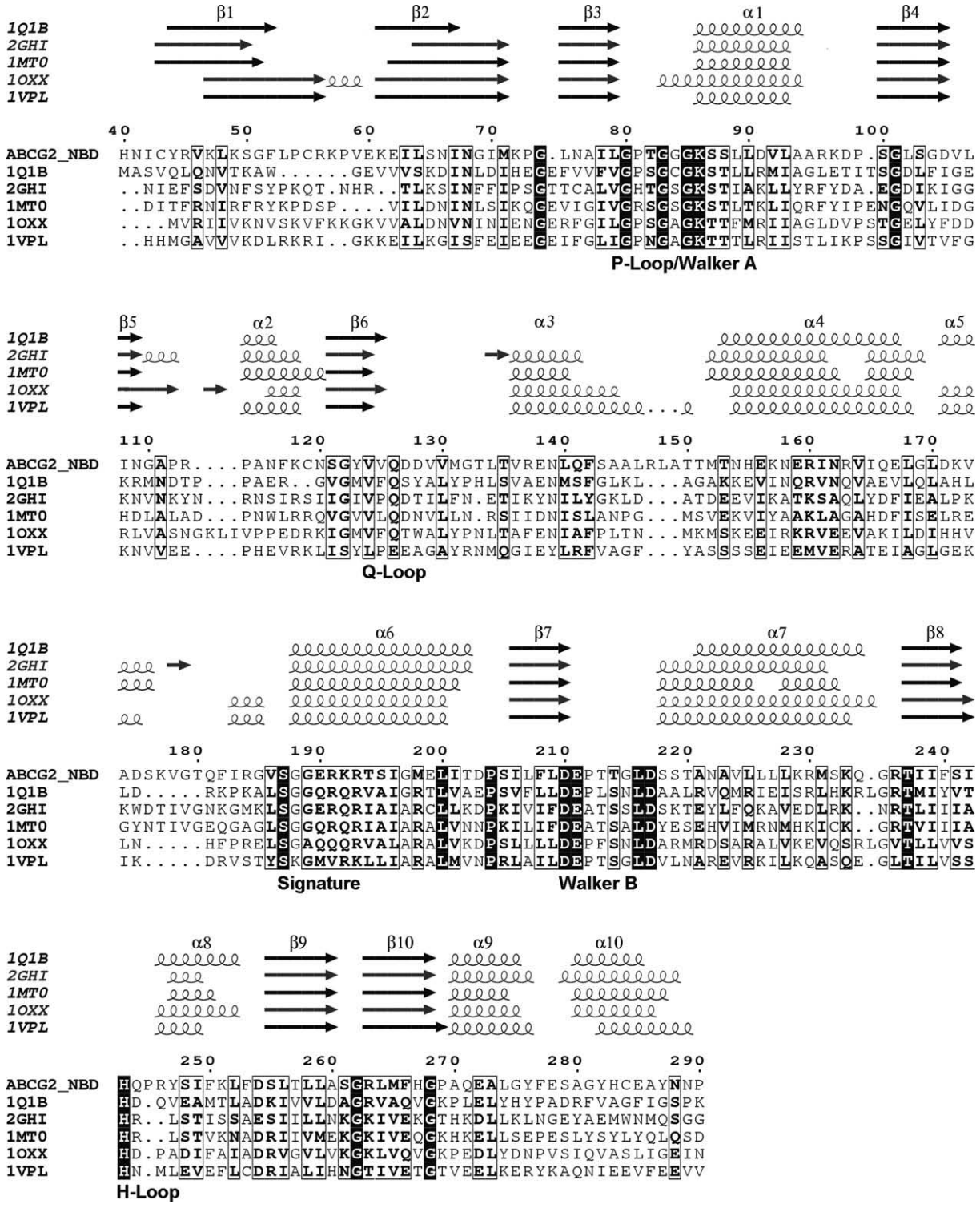

Fig. 2. Multiple sequence alignment of ABCG2 NBD and five templates. The nucleotide-binding domains of: *E. coli* Malk protein (PDB accession number 1Q1B), the *P. yoelii* MDR Protein 2 (PDB accession number 2GHI), the *E. coli* haemolysin B transporter (PDB accession number 1MT0), the *S. solfataricus* glucose ABC transporter (PDB accession number 1OXX) and the *T. maritima* ABC amino acid transporter (PDB accession number 1VPL). Arrows depict β-sheets and helices represent α-helices. Dots represent gaps within the secondary structure prediction. Black shaded blocks represent regions with identical amino acids and grey shaded blocks represent regions with similar amino acids.

Docking of ATP and MANT-ATP into the homology model of ABCB1 NBD2 predicted the molecules to occupy similar spatial locations within the NBD. The adenine rings of ATP and MANT-ATP were both predicted to interact with Tyr1044, whilst the α, β and γ phosphate groups of both molecules were predicted to form hydrogen bonds with several common amino acids (Table 1). The hydrophobic MANT moiety, however, was predicted to lie perpendicular to the plane of ATP and project into a hydrophobic cleft interacting with Ile1050 and Val1052 (Fig. 4a). Similar docking orientations of both ATP and MANT-ATP were also observed in the

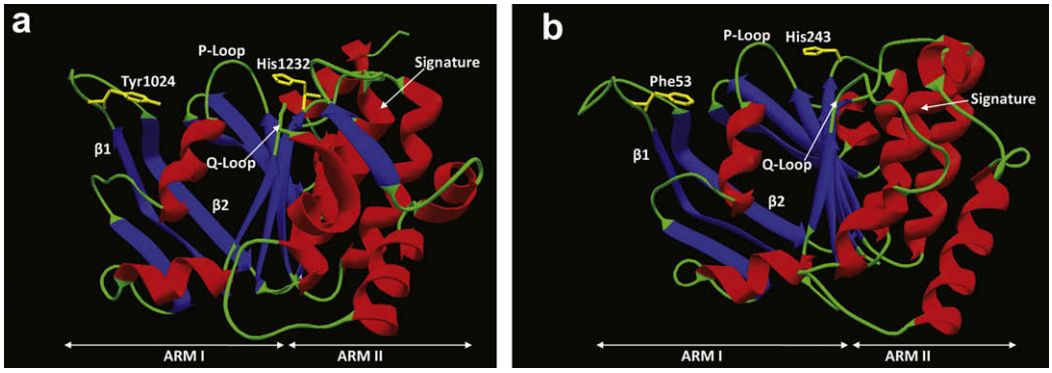

Fig. 3. (a) Homology model of ABCB1 NBD2, (b) homology model of ABCG2 NBD. α-Helices are illustrated in red and β-sheets in blue. (For interpretation of the references to colour in this figure legend, the reader is referred to the web version of this article.)

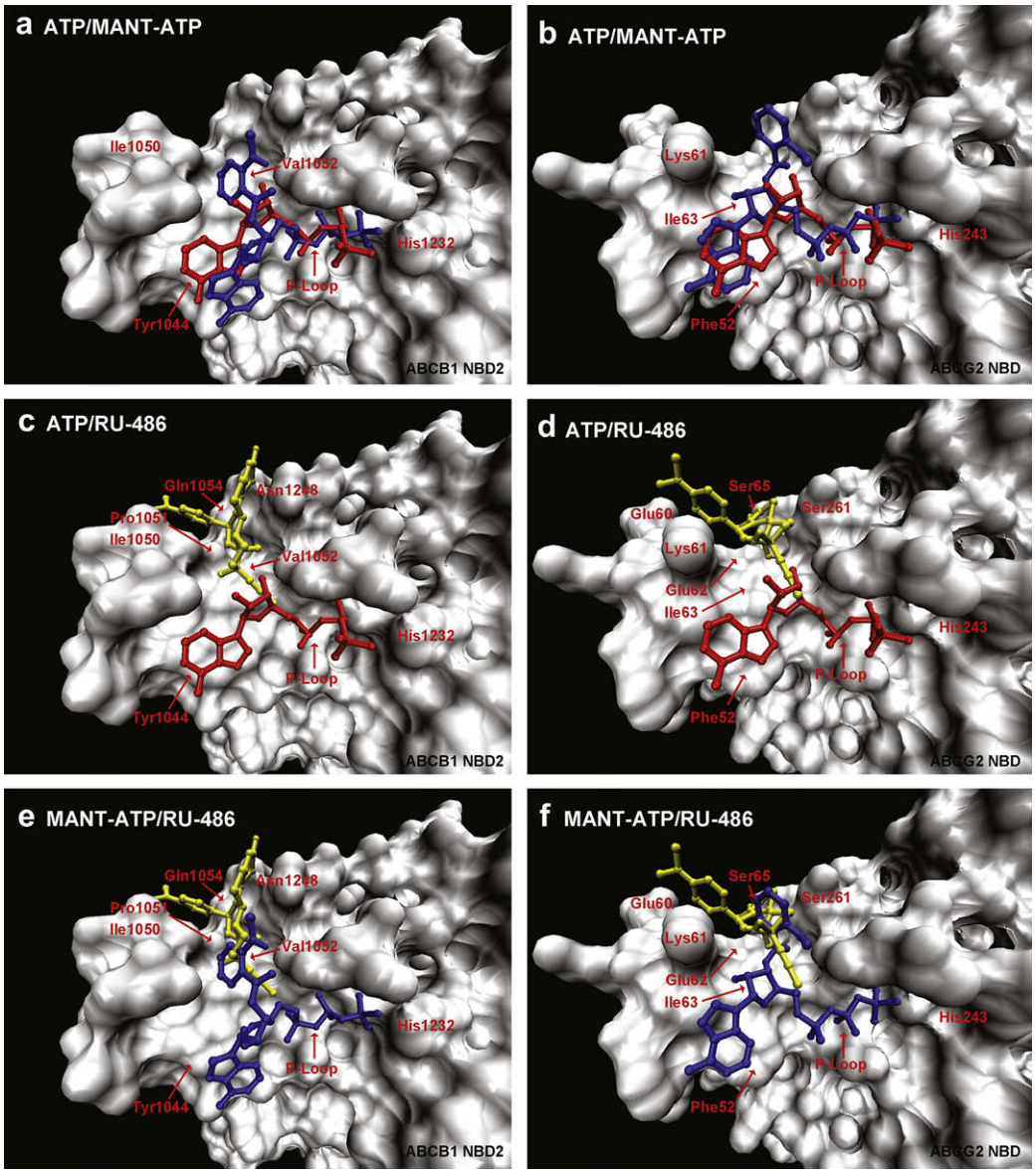

Fig. 4. Three-dimensional model of human ABCB1 NBD2 (a) and ABCG2 NBD (b) showing the docking orientation of ATP (red) and MANT-ATP (blue). Three-dimensional model of human ABCB1 NBD2 (c) and ABCG2 NBD (d) showing the docking orientation of ATP (red) and RU-486 (yellow). Docking orientation of MANT-ATP (blue) and RU-486 (yellow) in ABCB1 NBD2 (e) and ABCG2 NBD (f).

Table 1
Amino acids of ABCB1 NBD2 and ABCG2 NBD predicted to interact with steroids.

Compound	ABCB1 NBD2		ABCG2 NBD	
	Hydrophobic interaction	Hydrophilic interaction	Hydrophobic interaction	Hydrophilic interaction
Progesterone	Tyr1044, Ile1050, Val1052, Gly1073, Gly1075, Ser1077	Arg1047, Gln1085	Phe52, Lys61, Ile63, Gly83, Gly85	Glu62, Ser87
Dexamethasone	Tyr1044, Ile1050, Val1052, Gly1073, Gly1075, Ser1077	Lys1076	Phe52, Cys55, Ile63, Gly83, Gly85, Ser87	Lys61, Gly83, Ser87
Testosterone	Tyr1044, Ile1050, Val1052, Gly1075	Arg1047, Ser1077	Phe52, Cys55, Lys61, Glu62, Ile63, Ser261, Gly262	None predicted
Estradiol	Tyr1044, Val1052, Gly1075, Ser1077	Arg1047, Ser1077	Phe52, Cys55, Ile63, Gly83, Gly85	Lys61, Lys86, Ser87
Cortisol	Val1052, Cys1074, Gly1075, Lys1076, Ser1077	Arg1047, Gly1073	Phe52, Ile63, Gly83, Gly85	Gly83, Ser87
Corticosterone	Tyr1044, Ile1050, Val1052, Gly1075	Arg1047, Ser1077	Phe52, Lys61, Ile63, Gly85	Gly83, Ser87
Dihydrotes tosterone	Tyr1044, Ile1050, Val1052, Gly1075	Arg1047, Ser1077	Phe52, Cys55, Lys61, Glu62, Ile63, Ser261, Gly262	None predicted
Lanosterol	Tyr1044, Ile1050, Val1052, Gly1073, Gly1075, Ser1077, Asn1248, Gly1248	Pro1051	Phe52, Cys55, Ile63, Gly83, Gly85, Ser87, Ser88	Lys22
Pregnanedione	Tyr1044, Ile1050, Val1052, Gly1075,	Lys1076, Ser1077, His1232	Phe52, Ile63, Gly83, Gly85	Lys86, Ser87
Triamcinolone acetonide	Ile1050, Val1052, Gly1073, Gly1075, Ser1077	Arg1047, Lys1076, Ser1077	Ile63, Thr82, Gly83, Gly84, Gly85, Lys86	Ser87
ATP	Tyr1044, Gly1073	Gly1073, Cys1074, Gly1075, Ser1077, Thr1078	Phe52, Cys55, Ile63	Gly83, Gly84, Gly85, Lys86, Ser87, Ser88
MANT-ATP	Tyr1044, Ile1050, Val1052	Gly1073, Cys1074, Gly1075, Lys1076, Ser1077, Thr1078, Tyr1087	Phe52, Cys55, Lys61, Ile63	Gly83, Gly85, Lys86, Ser87, Ser88
RU-486	Ile1050, Pro1051, Val1052, Gln1054, Asn1248	None predicted	Glu60, Lys61, Glu62, Ile63, Ser65, Ser261	Arg263
Kaempferide	Tyr1044, Val1052, Gly1073, Gly1075	Arg1047, Ser1077, Thr1078	Phe52, Ile63, Thr82, Gly85	Gly83, Lys86, Ser87, Ser88

ABCG2 NBD homology model. The adenine rings of both ATP and MANT-ATP were predicted to interact with Phe52, Cys55 and Ile63, whilst the phosphate groups of both molecules were predicted to undergo hydrogen bonding with several common amino acids (Table 1). As was predicted with ABCB1 NBD2, the MANT moiety was perpendicular to the plane of ATP and projected into a hydrophobic region defined by Lys61 and Ile63 residues (Fig. 4b).

The highly hydrophobic steroid RU-486 has been reported to bind within the steroid-binding regions of abcb1 NBD1 [19] and abcb1 NBD2 [30]. Our docking studies show that, in the homology model of ABCB1, RU-486 was predicted to locate within the hydrophobic cleft defined by the Ile1050, Pro1051, Val1052 and Gln1054 residues (Fig. 4c). Moreover, RU-486 and ATP were predicted to interact with the NBD in such a manner that no significant overlap in binding sites was observed (Table 1). Similar results were obtained for ABCG2 NBD, whereby RU-486 was located within the hydrophobic region containing Lys61, Ile63 and Ser261 residues, with no significant overlap in ATP- and RU-486-binding sites predicted (Fig. 4d).

The MANT moiety of MANT-ATP and RU-486 are both hydrophobic in nature. Our simulations predicted both the MANT moiety and RU-486 to be located within the hydrophobic cleft composed of Ile1050 and Val1052 (Fig. 4e), indicating an overlap of MANT-ATP- and RU-486-binding sites within ABCB1 NBD2. Studies with ABCG2 NBD revealed similar findings whereby both the MANT moiety and RU-486 were predicted to be associated with a hydrophobic region of the protein containing Lys61 and Ile63 (Fig. 4f).

Several steroids (Fig. 5) have been reported to interact with the nucleotide-binding domain of abcb1, competing with, or displacing, ATP [19]. However, the precise locations and mechanisms of steroid interactions within nucleotide-binding domains have not been defined. To investigate the potential mechanisms of steroid-NBD interaction and identify putative steroid-binding sites, steroid-docking studies were performed with homology models of ABCB1 NBD2 and ABCG2 NBD.

In ABCB1 NBD2, the overall predicted docking orientations of all steroids (progesterone, dexamethasone, testosterone, estradiol, cortisol, corticosterone, dihydrotestosterone, lanosterol, pregnanedione and triamcinolone acetonide) were practically identical. Steroids were predicted to bind within a cavity formed partly by the P-Loop, with Tyr1044 and Ile1050 at opposite ends of the cavity (Fig. 6a and b).

Rings A and B of steroids were located in the environs of the P-Loop and were predicted to undergo hydrophobic interactions with Gly1075 located within the P-loop and with Tyr1044. Rings C and D were involved in hydrophobic interactions with Val1052 and Ile1050. Keto and hydroxyl groups associated with side chains at position 17 of ring D were predicted to interact with Arg1047 forming a hydrogen bond. Additional predicted hydrophobic and hydrophilic interactions are listed in Table 1.

The ATP- and steroid-binding sites within ABCB1 NBD2 are predicted to overlap in the vicinity of the P-Loop where both ATP and steroids interact with Val1052, Gly1075 and Ser1077. Both ATP and steroids are also predicted to interact with Tyr1044. The predicted free energy of docking of all steroids (between −5.96 and −7.06 kcal/mol) did not differ significantly from that of ATP, −5.88 kcal/mol (Table 2).

The predicted docking orientations of all steroids within the ABCG2 NBD homology model were almost invariant. All steroids were predicted to bind in the vicinity of the P-Loop (Fig. 6c and d). Rings C and D were predicted to undergo hydrophobic interactions with Phe52, Gly83 and Gly85. In addition, hydrophobic interactions were observed between rings A and B and Ile63. Although hydrophilic interactions were predicted between Ser87 and the keto and hydroxyl moieties at position 3 of ring A, such interactions were not predicted to occur with testosterone, dihydrotestosterone and lanosterol (Table 1).

The predicted docking orientation of progesterone within ABCB1 NBD2 is such that rings A and B of the steroid were situated in the vicinity of the P-Loop (Fig. 6a), undergoing hydrophobic interactions with Gly1073, Gly1075 and Ser1077 and also with Tyr1044. Rings C and D underwent hydrophobic interactions with Ile1050 and Val1052. Moreover, hydrophilic interactions were identified between the keto group at position 3 of ring A and Gln1081 of the P-Loop and between the keto group of the side chain at position 17 of ring D with Arg1047 (Table 1). The predicted free

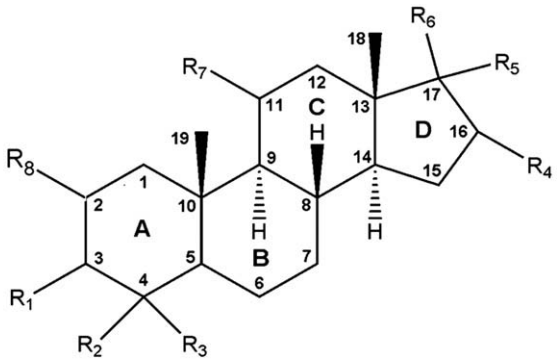

Compounds	Substituents								Double bond
	R_1	R_2	R_3	R_4	R_5	R_6	R_7	R_8	
Progesterone	=O	H	-	H	H	$COCH_3$	H	H	4
Dexamethasone	=O	H	-	CH_3	OH	$COCH_2OH$	OH	H	1,4
Testosterone	=O	H	-	H	H	OH	H	H	4
Estradiol	OH	H	-	H	H	OH	H	H	1,3,5
Cortisol	=O	H	-	H	OH	$COCH_2OH$	OH	H	4
Corticosterone	=O	H	-	H	H	$COCH_2OH$	OH	H	4
Dihydrotestosterone	=O	H	H	H	H	OH	H	H	-
Lanosterol	OH	CH_3	CH_3	H	H	$CHCH_3(CH_2)_2$-$CHC(CH_3)_2$	H	H	8
Pregnanedione	=O	H	H	H	H	CH_2CH_3	H	=O	-
Triamcinolone Acetonide	=O	H	-	OH	OH	O-$C(CH_3)_2$-O	OH	H	1,4
RU-486	=O	H	-	H	-C≡C-CH_3	OH	Ph-$N(CH_3)_2$	H	4,9

Fig. 5. Chemical structures of steroids docked into homology models of ABCB1 and ABCG2 nucleotide-binding domains.

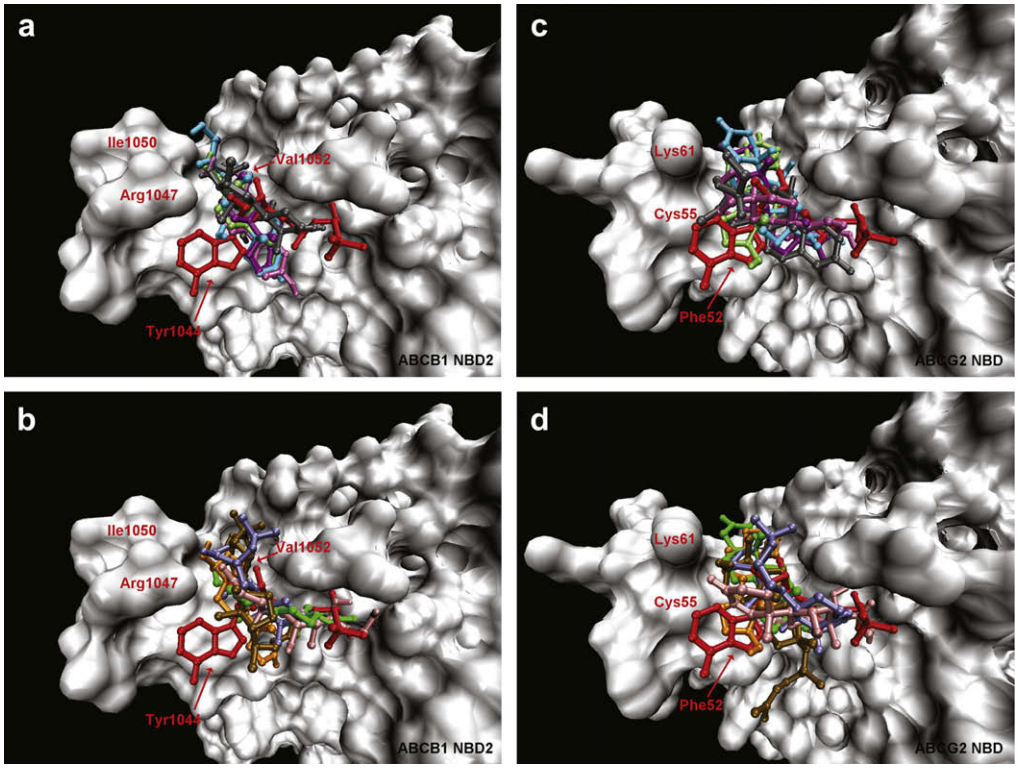

Fig. 6. Three-dimensional model of human ABCB1 NBD2 showing the docking orientation of (a) progesterone (purple), dexamethasone (grey), testosterone (light green), estradiol (dark pink), corticosterone (light blue) and (b) orientations of cortisol (light blue), dihydrotestosterone (orange), lanosterol (brown), pregnanedione (dark green) and triamcinolone (dark blue). Three-dimensional model of human ABCG2 NBD showing the docking orientation of (c) progesterone (purple), dexamethasone (grey), testosterone (light green), estradiol (dark pink), corticosterone (light blue) and (d) orientations of cortisol (light blue), dihydrotestosterone (orange), lanosterol (brown), pregnanedione (dark green) and triamcinolone (dark blue). ATP is shown in red. (For interpretation of the references to colour in this figure legend, the reader is referred to the web version of this article.)

Table 2
Predicted free energy of binding for compounds within ABCB1 and ABCG2 nucleotide-binding domains.

Compounds	E_B (kcal/mol)	Total cluster number	Energy range (kcal/mol)	Conformations within cluster	E_B (kcal/mol)	Total cluster number	Energy range (kcal/mol)	Conformations within cluster
Lanosterol	−7.06	13	−7.06 to −6.01	48	−6.98	17	−6.98 to −6.22	41
Pregnanedione	−6.7	6	−6.70 to −6.44	80	−6.31	2	−6.31 to −6.24	54
Cortisol	−6.57	11	−6.57 to −5.93	35	−6.02	20	−6.02 to −4.67	20
Triamcinolone acetonide	−6.47	12	−6.47 to −5.59	69	−5.39	8	−5.39 to −4.75	53
Progesterone	−6.42	4	−6.42 to −6.02	36	−6.7	1	−6.70 to −6.30	100
Corticosterone	−6.21	14	−6.21 to −6.03	24	−5.81	13	−5.81 to −5.04	28
Dihydrotestosterone	−6.12	4	−6.12 to −5.96	60	−5.64	2	−5.64 to −5.53	99
Testosterone	−6.07	5	−6.07 to −5.92	71	−5.64	3	−5.64 to −5.57	68
Dexamethasone	−5.96	20	−5.96 to −5.11	66	−5.21	16	−5.21 to −4.96	66
Estradiol	−5.54	10	−5.54 to 5.49	67	−5.59	2	−5.59 to −5.18	74
ATP	−5.88	6	−5.88 to −4.54	73	−9.24	2	−9.24 to −8.94	99
MANT-ATP	−7.85	9	−7.85 to −7.77	52	−7.43	5	−7.43 to −7.15	48
RU-486	−5.39	6	−5.39 to −5.13	15	−6.2	8	−6.2 to −6.03	26
Kaempferide	−5.28	20	−5.28 to −4.91	19	−5.09	12	−5.09 to −4.91	30

E_B: predicted free energy of binding.

energy of binding of progesterone to ABCB1 NBD2 was −6.42 kcal/mol.

Progesterone was predicted to interact with ABCG2 NBD at a binding pocket comprised of the P-Loop, Phe52 and Lys61 (Fig. 6c). Rings A, B and C were predicted to undergo hydrophobic interactions and Lys61 and Ile63. Rings C and D were located in the vicinity of the P-Loop and were predicted to undergo hydrophobic interactions with Phe52, Gly83 and Gly85. Furthermore, hydrogen bonding was predicted between the keto group of ring A at position 3 and Glu62 and between the keto group of the side chain at position 17 of ring D with Ser87 (Table 1). The predicted free energy of binding of progesterone to ABCG2 NBD was −6.7 kcal/mol (Table 1).

In ABCG2 NBD, an overlap in the predicted binding sites of ATP and steroids was observed. This overlap was evident in the vicinity of the P-Loop, where residues predicted to stabilise ATP, namely Phe52, Ile63 and Ser87, were also predicted to undergo hydrophobic and hydrophilic interactions with steroids (Table 1). The predicted free energy of binding of steroids to ABCG2 NBD ranges from −5.39 to −6.70 kcal/mol whilst that of ATP is −9.24 kcal/mol (Table 2).

Flavonoids possess structural similarities to both ATP and steroids and bind at the nucleotide-binding domain of abcb1. The binding sites of the flavone kaempferide and ATP were predicted to overlap, both compounds undergoing hydrophobic interactions with Tyr1044 and Gly1073 and forming hydrogen bonds with Ser1077 and Thr1078 in ABCB1 NBD2 (Fig. 7a, Table 1). In addition, the binding sites of kaempferide and MANT-ATP were predicted to overlap (Fig. 7b, Table 1) as were the binding sites of kaempferide and RU-486 (Fig. 7c, Table 1).

In ABCG2 NBD, kaempferide and ATP-binding sites were predicted to overlap, with both compounds undergoing hydrophobic interactions with Phe52 and Ile63 and hydrogen bond formation with Gly83, Lys86, Ser87 (Fig. 7d, Table 1). In addition, as observed with ABCB1 NBD2, the binding sites of kaempferide and MANT-ATP (Fig. 7e, Table 1) and of kaempferide and RU-486 (Fig. 7f, Table 1) were predicted to overlap.

3. Discussion

The homology-modelled nucleotide-binding domains of ABCB1 and ABCG2 exhibited high levels of sequence homology and possessed the same overall secondary structure topology as their respective crystal structure templates. The finding that 99.6% of ABCB1 NBD1 residues and 99.6% of ABCG2 NBD residues lie within allowed areas of Ramachandran plots suggest excellent structural similarities between homology models and crystal structure templates. Superimposing homology models of ATP-docked ABCB1 NBD2 and ABCG2 NBD on their respective templates co-crystallised with ATP revealed the orientation of the nucleotide within the homology models to be consistent with those within the crystal structures. These findings suggest the homology models are stereochemically robust and ligand docking reliable. A similar approach has been used to analyse potential mechanisms of interactions between flavonoids and recombinant abcb1 NBD and to correlate relative predicted docking energy with in vitro determined affinity [32].

Interaction of steroids with ABC transporter nucleotide-binding domain has been reported previously and may be rationalised by the fact that steroids possess structural similarities to the endogenous high affinity substrate, ATP. Moreover, these studies propose tentative relative locations of ATP- and steroid-binding sites within the nucleotide-binding domain. In an attempt to identify ATP- and potential steroid-binding sites within the NBDs of both ABCB1 and ABCG2, and establish the relative proximities of the sites, in silico docking of a series of steroids was carried out.

Many of the steroids (progesterone, dexamethasone, testosterone, cortisol, corticosterone, dihydrotestosterone, triamcinolone acetonide and RU-486) utilised in in silico docking studies have been shown to bind to recombinant murine abcb1 NBD1 [19]. RU-486, a highly hydrophobic steroid, was predicted to bind in a hydrophobic cleft in ABCB1 with no hydrophilic interactions observed. Similarly, RU-486 was predicted to undergo extensive hydrophobic interactions within a protein cleft within ABCG2, with only extremely limited hydrophilic interactions predicted. The hydrophobic protein domains in which RU-486 was predicted to bind appear to be distinct from the ATP-binding sites within both ABCB1 and ABCG2 since no overlap between binding sites was predicted. These findings are consistent with those of Dayan et al. [19] who report the interaction of RU-486 with recombinant nucleotide-binding domain was neither prevented nor reversed by high ATP concentrations. Despite no overlap in ATP- and RU-486-binding sites being predicted, we observed an overlap in MANT-ATP- and RU-486-binding sites in both ABCB1 NBD2 and ABCG2 NBD. This overlap between binding sites is also substantiated by Dayan et al. [19], who report the hydrophobic MANT moiety of the nucleotide analogue overlaps the proposed adjacent steroid-binding region at which RU-486 binds.

In both ABCB1 NBD2 and ABCG2 NBD, steroids other than RU-486 were also predicted to interact with amino acids within the vicinity of the hydrophobic clefts where RU-486 binds. In addition,

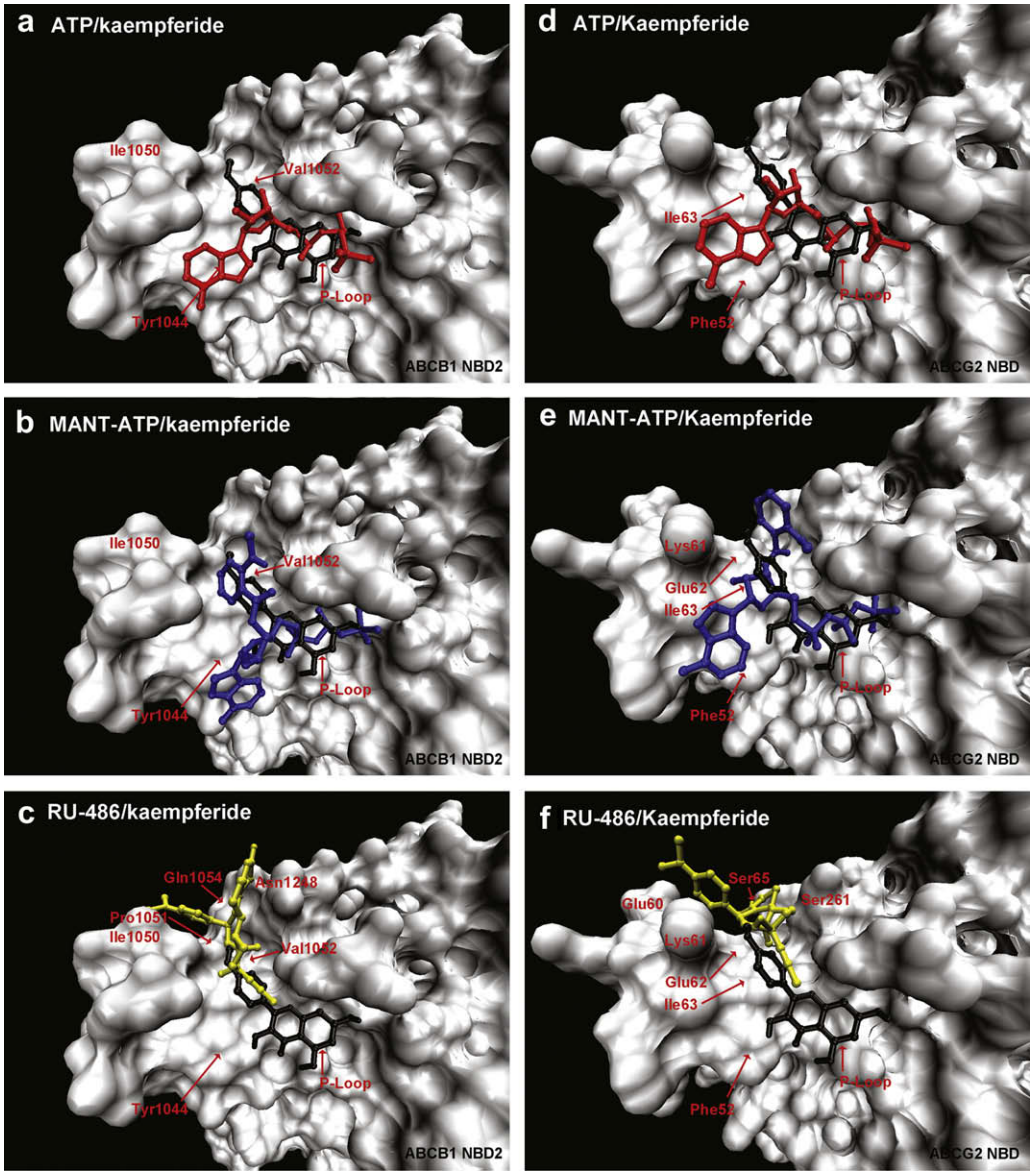

Fig. 7. Three-dimensional model of human ABCB1 NBD2 (a) and ABCG2 NBD (b) showing the docking orientation of ATP (red) and kaempferide (black). Three-dimensional model of human ABCB1 NBD2 (c) and ABCG2 NBD (d) showing the docking orientation of MANT-ATP (blue) and kaempferide (black). Docking orientation of RU-486 (yellow) and kaempferide (black) in ABCB1 NBD2 (e) and ABCG2 NBD (f). (For interpretation of the references to colour in this figure legend, the reader is referred to the web version of this article.)

these steroids were predicted to project towards the ATP-binding site. A direct comparison of binding sites of ATP and steroids other than RU-486 is not possible since Dayan et al. [19] did not investigate the effect of ATP on steroid-induced quenching for steroids other than RU-486. However, the study reports RU-486 binding to abcb1 NBD1 was substantially higher than the binding of all other steroids studied. A possible explanation for this may relate to different mechanisms of binding and/or different sites of interaction which are likely influenced by the physicochemical characteristics of the steroids.

In order to address the potential of compounds to interact at the ATP-binding site within an ABC transporter protein, the steroid-like flavone kaempferide was docked into NBD2 of the human ABCB1 transporter. In silico studies predicted a large overlap between ATP- and kaempferide-binding sites. In addition, overlaps between kaempferide-RU-486-binding sites and kaempferide-MANT-ATP-binding sites were predicted. These findings are consistent with those of Conseil et al. [30] who demonstrated kaempferide bound with relatively high affinity to hexahistidine-tagged murine NBD2 with binding being partially prevented by preincubation with ATP, or partly displaced following addition of ATP. In addition, these studies report kaempferide partially prevented the binding of RU-486 to a hydrophobic region located close to the ATP site and that MANT-ATP binding was completely prevented or displaced by kaempferide.

The findings of in silico docking studies aimed at better defining ATP- and steroid-binding sites within the NBDs of human ABC transporters are consistent with independent in vitro studies employing recombinant abcb1 NBD1, extended-NBD1 and NBD2 [19,30,31]. These studies have contributed to defining the potential mechanisms of steroid–protein interaction and identifying putative steroid-binding sites within ABCB1 NBD2 and ABCG2 NBD.

4. Conclusion

Inhibition of ABC transporter-mediated drug efflux has the potential to impact on the success of many disease treatments. Transporter inhibition can result in more efficient absorption of orally administered drugs, increased delivery of therapeutics to the central nervous system and increased intracellular drug accumulation in multidrug resistant malignant cells over-expressing drug efflux transporters. Consequently, there is an undisputed requirement to develop new agents that block ABC transporter-mediated drug efflux. Factors including the substrate-induced fit model reflecting plasticity of drug-binding sites and the potential for simultaneous binding of more than one substrate molecule mean design of transporter modulators directed to the transmembrane domains is extremely challenging. Since NBD function is critical for substrate transport, targeting these domains is an extremely attractive strategy for potentially counteracting drug efflux. Despite there being conserved motifs within the nucleotide-binding domains, regions of sequence diversity are also apparent and represent potential targets for de novo drug design. Therefore, understanding the structural requirements for, and mechanistics of interaction of compounds with NBDs may prove useful in developing more effective modulators targeted to ABC transporter proteins.

5. Experimental protocols

5.1. Model building

Suitable template proteins for the modelling of ABCB1 NBD2 and ABCG2 NBD were identified by means of a BLAST search [33]. The search was filtered for known 3D structures and five templates selected. Crystallographic structures of templates were obtained from the Protein Data Bank [34]. Multiple amino acid sequence alignments of target and template proteins were generated using ClustalW maintaining the default parameters [35]. Alignments were inspected and adjusted manually to minimise the number of gaps and insertions and to conserve the secondary structure of the templates. The secondary structures of the templates were designated using the ESPRIPT programme [36]. Homology models were generated using Modeller 9 Version 1 software [37]. Refinement of models was carried out using loop optimisation within Modeller 9.1. Optimal models were selected based on bond angle stereochemistry by means of the analysis of Ramachandran plots, which were obtained by submitting homology models to the Molprobity server [38].

5.2. Docking simulation studies

The binding orientations of ATP and steroids in homology models were analysed using AutoDock 4.0.1 [39,40] and the graphical interface AutoDock Tools 1.4.5 [41]. Two-dimensional steroid structures were generated using ChemDraw Ultra Version 10.0 (CambridgeSoft 2005). Structures were submitted to the Dundee PRODRG2 server [42] to obtain three-dimensional coordinates (PDB format), to assign partial charges and to perform energy minimisations. Polar hydrogens and non-polar hydrogens were added and Gasteiger charges computed using AutoDock Tools.

The grid volume was set up to cover a three-dimensional analysis region of 76 Å × 56 Å × 42 Å with a grid spacing of 0.375 Å. The three-dimensional region was centred on the P-Loop. The grid volume was large enough to allow the ligand to rotate freely, even when the ligand was in its most fully-extended conformation. Docking was carried out using the hybrid Lamarckian Genetic Algorithm with 100 runs per ligand and 2,500,000 energy evaluations. All other parameters were maintained at their default settings. Cluster analysis was performed on the docked results using a root mean square deviation (RMSD) tolerance of 0.5 Å.

Hydrogen bonding and hydrophobic interactions between docked molecules and amino acid residues within ABCB1 NBD2 and ABCG2 NBD models were determined using LIGPLOT v.4.0 [43]. Molecular surface representations were generated using Visual Molecular Dynamics [44] and SwissPdb Viewer v3.7 [45].

Acknowledgments

Funding support by The Mexican Council for Science and Technology (CONACyT) is gratefully acknowledged.

References

[1] T.R. Stouch, O. Gudmundsson, Adv. Drug. Deliv. Rev. 54 (2002) 315–328.
[2] L.A. Doyle, W. Yang, L.V. Abruzzo, T. Krogmann, Y. Gao, A.K. Rishi, D.D. Ross, Proc. Natl. Acad. Sci. U.S.A. 95 (1998) 15665–15670.
[3] T. Litman, M. Brangi, E. Hudson, P. Fetsch, A. Abati, D.D. Ross, K. Miyake, J.H. Resau, S.E. Bates, J. Cell Sci. 113 (2000) 2011–2021.
[4] C. Ozvegy, T. Litman, G. Szakacs, Z. Nagy, S. Bates, A. Varadi, B. Sarkadi, Biochem. Biophys. Res. Commun. 285 (2001) 111–117.
[5] T. Ando, H. Kusuhara, G. Merino, A.I. Alvarez, A.H. Schinkel, Y. Sugiyama, Drug Metab. Dispos. 35 (2007) 1873–1879.
[6] C. Cordon-Cardo, J.P. O'Brien, J. Boccia, D. Casals, J.R. Bertino, M.R. Melamed, J. Histochem. Cytochem. 38 (1990) 1277–1287.
[7] M. Maliepaard, G.L. Scheffer, I.F. Faneyte, M.A. van Gastelen, A.C. Pijnenborg, A.H. Schinkel, M.J. van De Vijver, R.J. Scheper, J.H. Schellens, Cancer Res. 61 (2001) 3458–3464.
[8] H.C. Cooray, C.G. Blackmore, L. Maskell, M.A. Barrand, Neuroreport 13 (2002) 2059–2063.
[9] A. Ahmed-Belkacem, A. Pozza, S. Macalou, J.M. Perez-Victoria, A. Boumendjel, A. Di Pietro, Anticancer Drugs 17 (2006) 239–243.
[10] T. Mizutani, A. Hattori, Drug. Metab. Rev. 37 (2005) 489–510.
[11] E.M. Leslie, R.G. Deeley, S.P. Cole, Toxicol. Appl. Pharmacol. 204 (2005) 216–237.
[12] I. Klein, B. Sarkadi, A. Varadi, Biochim. Biophys. Acta 1461 (1999) 237–262.
[13] P.M. Jones, A.M. George, FEMS Microbiol. Lett. 179 (1999) 187–202.
[14] P. Manavalan, D.G. Dearborn, J.M. McPherson, A.E. Smith, FEBS Lett. 366 (1995) 87–91.
[15] K. Ueda, N. Okamura, M. Hirai, Y. Tanigawara, T. Saeki, N. Kioka, T. Komano, R. Hori, J. Biol. Chem. 267 (1992) 24248–24252.
[16] D.C. Wolf, S.B. Horwitz, Int. J. Cancer 52 (1992) 141–146.
[17] K.M. Barnes, B. Dickstein, G.B. Cutler Jr., T. Fojo, S.E. Bates, Biochemistry 35 (1996) 4820–4827.
[18] D.J. Gruol, M.C. Zee, J. Trotter, S. Bourgeois, Cancer Res. 54 (1994) 3088–3091.
[19] G. Dayan, J.M. Jault, H. Baubichon-Cortay, L.G. Baggetto, J.M. Renoir, E.E. Baulieu, P. Gros, A. Di Pietro, Biochemistry 36 (1997) 15208–15215.
[20] L. Schmitt, H. Benabdelhak, M.A. Blight, I.B. Holland, M.T. Stubbs, J. Mol. Biol. 330 (2003) 333–342.
[21] Y. Yuan, H. Chen, D. Patel, Crystal structure of LmrA ATP-binding domain reveals the two-site alternating mechanism at molecular level. Protein Data Bank Accession Code: 1mv5.
[22] M. Vedadi, J. Lew, J. Artz, M. Amani, Y. Zhao, A. Dong, G.A. Wasney, M. Gao, T. Hills, S. Brokx, W. Qiu, S. Sharma, A. Diassiti, Z. Alam, M. Melone, A. Mulichak, A. Wernimont, J. Bray, P. Loppnau, O. Plotnikova, K. Newberry, E. Sundararajan, S. Houston, J. Walker, W. Tempel, A. Bochkarev, I. Kozieradzki, A. Edwards, C. Arrowsmith, D. Roos, K. Kain, R. Hui, Mol. Biochem. Parasitol. 151 (2007) 100–110.
[23] E. Procko, I. Ferrin-O'Connell, S.L. Ng, R. Gaudet, Mol. Cell 24 (2006) 51–62.
[24] R. Gaudet, D.C. Wiley, EMBO J. 20 (2001) 4964–4972.
[25] J. Chen, G. Lu, J. Lin, A.L. Davidson, F.A. Quiocho, Mol. Cell 12 (2003) 651–661.
[26] G. Verdon, S.V. Albers, N. van Oosterwijk, B.W. Dijkstra, A.J. Driessen, A.M. Thunnissen, J. Mol. Biol. 334 (2003) 255–267.
[27] Joint-Center-for-Structural-Genomics, Crystal structure of ABC transporter ATP-binding protein (TM0544) from *Thermotoga maritima* at 2.10 Å resolution. Protein Data Bank Accession Code: 1VPL.
[28] B. Rost, Protein Eng. 12 (1999) 85–94.
[29] G. Lu, J.M. Westbrooks, A.L. Davidson, J. Chen, Proc. Natl. Acad. Sci. U.S.A. 102 (2005) 17969–17974.
[30] G. Conseil, H. Baubichon-Cortay, G. Dayan, J.M. Jault, D. Barron, A. Di Pietro, Proc. Natl. Acad. Sci. U.S.A. 95 (1998) 9831–9836.
[31] G. Dayan, H. Baubichon-Cortay, J.M. Jault, J.C. Cortay, G. Deleage, A. Di Pietro, J. Biol. Chem. 271 (1996) 11652–11658.
[32] R. Badhan, J. Penny, Eur. J. Med. Chem. 41 (2006) 285–295.
[33] S.F. Altschul, T.L. Madden, A.A. Schaffer, J. Zhang, Z. Zhang, W. Miller, D.J. Lipman, Nucleic Acids Res. 25 (1997) 3389–3402.
[34] H.M. Berman, J. Westbrook, Z. Feng, G. Gilliland, T.N. Bhat, H. Weissig, I.N. Shindyalov, P.E. Bourne, Nucleic Acids Res. 28 (2000) 235–242.

[35] J.D. Thompson, D.G. Higgins, T.J. Gibson, Nucleic Acids Res. 22 (1994) 4673–4680.
[36] P. Gouet, X. Robert, E. Courcelle, Nucleic Acids Res. 31 (2003) 3320–3323.
[37] M. Topf, M.L. Baker, M.A. Marti-Renom, W. Chiu, A. Sali, J. Mol. Biol. 357 (2006) 1655–1668.
[38] I.W. Davis, A. Leaver-Fay, V.B. Chen, J.N. Block, G.J. Kapral, X. Wang, L.W. Murray, W.B. Arendall 3rd, J. Snoeyink, J.S. Richardson, D.C. Richardson, Nucleic Acids Res. 35 (2007) W375–W383.
[39] G.M. Morris, D.S. Goodsell, R. Huey, A.J. Olson, J. Comput. Aided Mol. Des. 10 (1996) 293–304.
[40] R. Huey, G.M. Morris, A.J. Olson, D.S. Goodsell, J. Comput. Chem. 28 (2007) 1145–1152.
[41] M.F. Sanner, B.S. Duncan, C.J. Carrillo, A.J. Olson, Pac. Symp. Biocomput. (1999) 401–412.
[42] A.W. Schuttelkopf, D.M. van Aalten, Acta Crystallogr. D: Biol. Crystallogr. 60 (2004) 1355–1363.
[43] A.C. Wallace, R.A. Laskowski, J.M. Thornton, Protein Eng. 8 (1995) 127–134.
[44] W. Humphrey, A. Dalke, K. Schulten, J. Mol. Graph. 14 (1996) 33–38 27–38.
[45] N. Guex, M.C. Peitsch, Electrophoresis 18 (1997) 2714–2723.